Arabian Journal of Chemical and Environmental Research Vol. 13 Issue 1 (2026) 1–17



Synthesis and characterization of activated carbon from agricultural waste

Abdullahi Yusuf^{1*}, Murtala Maidamma Ambursa², Aminu Koko Rabi'u³

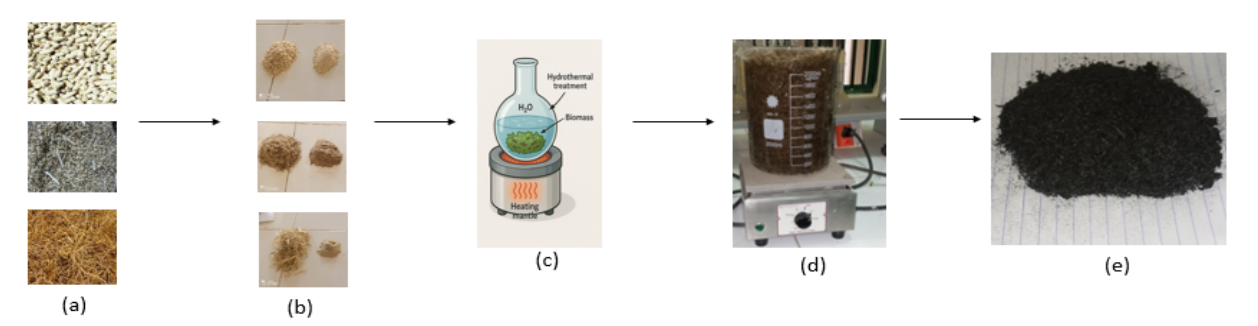
1,2,3: Department of Pure and Industrial Chemistry, Abdullahi Fodio University of Science & Technology, Aliero, Kebbi State, Nigeria

murtalamaidamma79@gmail.com arkoko2003@gmail.com

Received 01 November 2025, Revised 10 Oct 2025, Accepted 14 Oct 2025

Cited as: Abdullahi Yusuf, Murtala M. Ambursa and Aminu K. Rabi'u (2026) Synthesis and Characterization of Activated Carbon from Agricultural Waste, Arab. J. Chem. Environ. Res. 13(1), 1-17

Graphical Abstract



- a. Raw Corn Cob, Millet Husk and Rice Straw
- b. After crushing and grinding
- c. Hydrothermal treatment using H_2O
- d. Chemical Activation using (H2SO4, NaOH, ZnCl2)
- e. Activated Carbon after Carbonization

Abstract

This study investigated the synthesis of activated carbon from corn cob (CC), millet husk (MH), and rice straw (RS) as sustainable, low-cost adsorbents for environmental and industrial use. A two-step hydrothermal pretreatment followed by chemical activation with H₂SO₄, HNO₃ and ZnCl₂ was applied under optimized conditions of temperature and time. Differential Thermal Analysis (DTA) showed multi-stage decomposition with high mass losses (93% CC, 77% MH, 85% RS). Activation at lower temperatures (150 °C) with longer times (120 min) generally improved yield, with Corn Cob Activated Carbon (CCAC) H₂SO₄ giving the highest yield (43.2 g). Proximate analysis revealed low moisture (3.4-4.2%) and high fixed carbon (up to 82.4%) in CCAC, while Rice Straw Activated Carbon (RSAC)

ISSN: 2458-6544 © 2026; www.mocedes.org. All rights reserved.

showed higher ash (13.14%) and lower fixed carbon (68.7-72.4%). Porosity studies indicated that HNO₃ activation produced the highest BET surface areas: 556.5 m²/g (CCAC), 387.0 m²/g Millet Husk Activated Carbon (MHAC), and 434.7 m²/g (RSAC). Iodine numbers confirmed superior microporosity in CCAC H₂SO₄ (1,223.5 mg/g) and MHAC H₂SO₄ (1,154.8 mg/g). SEM images displayed irregular porous structures, and FTIR identified functional groups (O-H, C=O, C-O, C=N) linked to surface reactivity. pH values varied with activating agents ranging from acidic (4.4 MHAC H₂SO₄) to near-neutral (7.5 RSAC ZnCl₂).

Keywords: Activated Carbon, Corn Cob, Millet Husk, Rice Straw, Optimization

Corresponding Author Email: abdollahiyusuf@gmail.com

1. Introduction

Heavy metal contamination of soil is one of the most pressing concerns in the world and this is about food safety and food security (Toth *et al.*, 2016; Karim *et al.*, 2019). Heavy metals, dyes and other pollutants cause food safety risks by introducing toxic metals into the food chain, which can then accumulate in human, animal and fish tissues, leading to various organ damages and health problems (Abdel-Rahman *et al.*, 2022; Sabbahi *et al.*, 2022; Angon et al., 2024). In recent years, the use of low-cost and waste abundant materials such as agricultural by-products in production of activated carbon have received much attention due to the high cost of commercially activated carbon produced from coal, woods among other sources (Baker 2018). Agricultural waste is a general term for organic substances discarded by human in the process of agricultural practices. It broadly contains plant waste, livestock and poultry waste and agricultural processing waste (Altenor 2009). Example of plant and agricultural processing waste includes: saw dust of various plants, bark of trees, leaves of trees, husk of millet, wheat, rice etc., shells of coconut, groundnut, walnut etc., stalks of millet, corn, grapes, olive, sun flower, cotton etc., straws of wheat, rice, barley etc., others include sugarcane bagasse, orange peels, corn cob among others (Tsade *et al.*, 2020; Konan *et al.*, 2020; Salahat *et al.*, 2023; Shah *et al.*, 2025).

In the new global economy, agricultural waste is considered to be very important feedstock due to their renewable source, carbon rich, low cost, abundance, besides contains high concentration of volatiles and low ash content which will favor the production of highly porous structure within activated carbon matrix beside they have little or no economic value and often pose a disposal problem (Opia *et al.*, 2020). Utilization of cheap and abundant raw materials in the production of adsorbents such as activated carbon will minimize cost of its production and will equally reduce solid waste pollution. Paddy rice, maize and millet are among of the major food plants produce in Nigeria which besides producing grains, also resulting in rice straw, corn cob as well as millet husk as by-product respectively

(Nguyen *et al.*, 2013; Akartasse *et al.*, 2022). The burning of this agricultural waste will convert organic components into carbon dioxide, air and ash. The ashes produce can be used as activate carbon which has been used as industrial filters, water purification, soil remediation among others.



Fig 1. (a) MH (b) CC (c) RS (d), (e) and (f) CC, MH and RS at crushin, grinding, hydrothermal treatment, chemical treatment and carbonization stages respectively

2. Methods

The Thermogravimetric Analyzer (TGA) were first employed to study the thermal behaviour of the samples. Synthesis was carried out according to the method reported by Adekola *et al.*, (2017) with some modifications. The collected samples were washed with clean water for removing any impurities, dust, filth particles or other fine dirt particles that may be stocked in the surface of the samples. The washed samples were sun dried for three days before subjecting to crushing using local pestle and mortar. In order to increase surface area of the samples, the samples were further grinded using blender until tiny particles were formed. The samples were later subjected to hydrothermal pretreatment under heating plate using water at 200°C for 3 hours. Further, chemical activation and carbonization was carried out according to factorial experimental design by Minitab statistical software version 19 with activation temperature, activation time, concentration of activation agent, carbonization temperature and carbonization time under investigation. The yield of the activated carbon was calculated using the formular:

Yield (%) =
$$\frac{initial\ weight\ of\ the\ sample}{final\ weight\ of\ activated\ carbon}\ X\ 100$$
 eqn. (1)

2.1 Characterization of Activated Carbon

Moisture Content were determined according to ASTM D2867, Ash Content: ASTM D2867-17, Volatile Organic Matter: ASTM D5832-98, Ph: ASTM D3838, Iodine Number: ASTM D4607-14. Other analysis carried out included BET, SEM and FTIR.

3. Results and discussion

Figure 2 a, b and c presents result DTA results of Corn Cob, Millet Husk and Rice Straw respectively. TGA is a vital analytical method for examining the thermal decomposition behavior of lignocellulosic biomass, particularly its key components: cellulose, hemicellulose and lignin. Studies reveal outlined thermal decomposition typically occurs in three distinct stages namely: drying, pyroletic and carbonization stages (Vassilev *et al.*, 2010). The drying stage (30°C -170 °C), this phase is primarily associated with the evaporation of moisture and the release of light volatiles or extractives. Across all the samples, a minor weight loss of 2 - 4% were observed. For pyrolytic stage (200 °C - 500 °C), major thermal degredation of organic components with significant mass loss due to decomposition of hemicellulose, cellulose and partial lignin were observed with corn cob, millet husk and rice straw exhibited weight loss of 93%, 77% and 85% respectively.

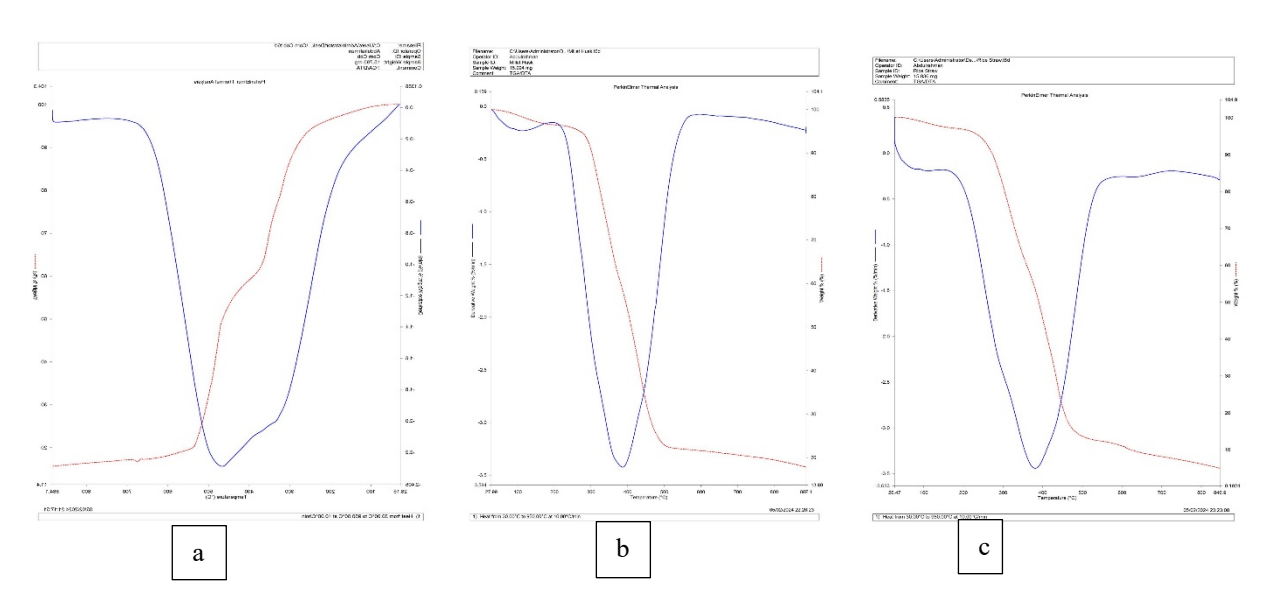


Fig 2. (a) DTA of Corn Cob (b) DTA of Millet Husk (c) DTA of Rice Straw

The sharp endothermic peaks on the DTA curves especially between 370 - 500 °C further confirmed intense decomposition with peak weight loss nearing 95-96%. Carbonization stage (>500 °C), beyond 500 °C, all samples showed negligible or no further weight loss thus indicating complete thermal

decomposition and transition of fixed carbon. The observed thermal patterns are consistent with previous findings by Gonzalez *et al.*, (2009) and Chen *et al.*, (2017).

Table 1. Optimization result for CCAC

Run	Activation	Activation	Concentration	Carbonization	Carbonization	Yield	Yield	Yield
order	temp. (°C)	time	(m)	temp. (°C)	time (min.)	(g)	(g)	(g)
		(min.)				H ₂ SO ₄	HNO ₃	Zncl ₂
1	150	120	8	450	30	43.2	38.7	32.7
2	300	60	4	450	30	38.9	40.2	34.1
3	300	120	4	550	30	37.4	35.3	37.8
4	150	60	4	550	60	39.6	39.8	31.4
5	300	60	8	450	60	40.2	36.8	29.7
6	150	120	4	450	60	36.8	41.3	33.8
7	300	120	8	550	60	41.2	37.5	40.3
8	150	60	8	550	30	38.5	38.2	42.6

Table 1, presented results of optimization studies in the production of activated carbon from CC, MH, and RS using chemical activating agents H₂SO₄, ZnCl₂, and HNO₃. The parameters examined included activation temperature, time, acid concentration, carbonization temperature, and carbonization time, all of which significantly influenced the product yield and quality. For CCAC, it was observed that lower activation temperatures (150°C) produced the highest yields across all activating agents, with H₂SO₄ yielding the most (43.2 g) which could be as a result of minimal thermal degradation and mass retention. This aligns with the findings of Lua and Yang (2014), who emphasized the role of activation temperature in determining the structural and functional properties of activated carbon. Longer activation times (120 min) at these lower temperatures also favored higher yields, supporting Ahmed and Theydan (2012) who noted the benefit of extended agent biomass interaction for maximizing output. Higher acid concentrations (8 M) generally improved yield (e.g., 43.2 g for H₂SO₄ and 40.3 g for ZnCl₂), consistent with El-Sayed and Bandosz (2015) who observed that increased acid strength promotes dehydration and charring. However, excessive concentration may reduce structural stability (Sun et al., 2018). Optimal carbonization occurred at 450°C for H₂SO₄ and HNO₃ and at 550°C for ZnCl₂, supporting the balance between porosity development and mass retention described by Nisar et al., (2020). Additionally, shorter carbonization times (30 min) enhanced yield by minimizing thermal decomposition, as noted by Zhang et al., (2023).

Table 2. Optimization Result for MHAC

Run	Activation	Activation	Concentration	Carbonization	Carbonization	Yield	Yield	Yield
Order	Temp.	Time	(M)	Temp. (°C)	Time (min.)	(g)	(g)	(g)
	(°C)	(min.)				H ₂ SO ₄	HNO ₃	ZnCl ₂
1.	300	120	4	400	30	27.3	28.7	25.4
2.	300	120	8	400	60	29.6	30	28.1
3.	300	60	8	350	60	28.1	26.9	26.5
4.	150	120	4	350	60	26.6	25.3	25.9
5.	300	60	4	350	30	27.9	27	28.3
6.	150	120	8	350	30	33	32.3	31.1
7.	150	60	4	400	60	31.4	33.1	30.6
8.	150	60	8	400	30	27.2	26.2	26.3

MHAC in **table 2**, indicated how low activation temperatures (150°C) yielded the best results across agents H₂SO₄ (33 g), HNO₃ (33.1 g), and ZnCl₂ (31.1 g). This is in concordance with findings of Akinyemi and Okon (2021) who noted that lower temperatures preserve the carbon structure. However, some studies suggest higher temperatures promote pore development at the expense of yield (Sulaiman and Rashid, 2020). Optimal activation times were 120 min for H₂SO₄ and ZnCl₂, but only 60 min for HNO₃, reflecting differences in agent-biomass interaction kinetics (Ojedokun and Bello, 2019). Higher concentrations (8 M) improved yield for H₂SO₄ and ZnCl₂ but were detrimental for HNO₃, where moderate concentrations (4 M) were optimal. This aligns with El-Sayed and Bandosz (2015), who emphasized that HNO₃ oxidative nature enhances porosity but may cause degradation at high concentrations. Carbonization at 350°C (for H₂SO₄ and HNO₃) and 400°C (for ZnCl₂) achieved the best yield structure balance (Nisar *et al.*, 2020), while 30 - 60 min. durations provided sufficient volatile removal with minimal degradation (Gupta *et al.*, 2015).

For RSAC in **Table 3**, all activating agents produced the highest yields at lower temperatures (150°C), with H₂SO₄ yielding 28.2 g, HNO₃ 27.9 g, and ZnCl₂ 26.4 g. This confirms the findings of Sulaiman and Rashid (2020), who indicated that mild temperatures stabilize biomass and minimize mass loss. Activation times of 120 min across all agents led to improved agent-biomass interaction and pore development, as reported by Li *et al.*, (2016).

Table 3. Optimization Result of RSAC

Run	Activation	Activation	Concentration	Carbonization	Carbonization	Yield	Yield	Yield
Order	Temp. (°C)	Time	(M)	Temp. (°C)	Time (min.)	(g)	(g)	(g)
		(min.)				H ₂ SO ₄	HNO ₃	ZnCl ₂
1	150	120	8	350	30	23.7	22.8	23.2
2	300	60	4	350	30	26.3	25.1	24.7
3	300	120	4	400	30	25.6	25.8	25
4	150	60	8	400	30	26	24.4	23.1
5	150	120	4	350	60	28.2	27.9	26.4
6	300	120	8	400	60	24.3	23	21.6
7	150	60	4	400	60	24.9	23.8	23.6
8	300	60	8	350	60	27.8	25.9	24.8

In contrast to other biomasses, higher activating agent concentrations (8 M) reduced RSAC yields, likely due to over aggressive chemical reactions. Lower concentrations (4 M) yielded better results, in line with Mahmoud *et al.*, (2018) who reported that mild chemical conditions prevent structural collapse. Carbonization at 350°C offered the best yield to structure performance, whereas 400°C caused pore collapse (Cheng *et al.*, 2017). Extended carbonization times (60 min) were optimal for volatile removal and structural stability (Akinyemi and Okon, 2021).

Table 4. Proximate Analysis

Sample	Moisture Content	Volatile Matter	Ash	Fixed Carbon
CCAC H ₂ SO ₄	3.7	6.3	7.5	82.4
CCAC HNO ₃	4.2	7.4	8.4	80.0
CCAC ZnCl ₂	3.4	7.6	8.7	80.3
MHAC H ₂ SO ₄	5.62	8.20	13.14	77.86
MHAC HNO ₃	6.10	7.3	7.18	79.42
MHAC ZnCl ₂	4.81	6.93	7.14	81.12
RSAC H ₂ SO ₄	6.8	9.3	13.14	70.76
RSAC HNO ₃	7.12	10.31	10.16	72.41
RSAC ZnCl ₂	6.81	12.42	12.06	68.71

Table 4, presented proximate analysis of the AC produced. Moisture content is a key parameter affecting the adsorption efficiency of activated carbon. In this study, CCAC showed the lowest moisture content (3.4-4.2%), indicating higher thermal stability and lower hydrophilicity, especially with ZnCl₂

activation, which promotes effective dehydration (Ahmed & Theydan, 2012; El-Sayed & Bandosz, 2015). MHAC exhibited moderate moisture levels (4.81-6.10%), possibly due to its fibrous and less dense nature (Akinyemi & Okon, 2021). RSAC had the highest moisture content (6.8-7.12%), attributed to its porous, hydrophilic structure and oxygenated surface groups introduced by HNO₃ treatment (Sun *et al.*, 2018).

CCAC volatile organic matter content was lowest in H₂SO₄ (6.3%) and highest in ZnCl₂ (7.6%). While MHAC volatile organic matter content ranged from 6.93% (ZnCl₂) to 8.20% (H₂SO₄) indicating moderate carbonization efficiency. For RSAC, volatile organic matter content was highest ranging from 9.3% (H₂SO₄) to 12.42% (ZnCl₂) suggesting retention of organic residues. This therefore concluded CCAC had the lowest volatile organic matter particularly with H₂SO₄ activation hence suggesting superior thermal stability. RSAC exhibited the highest volatile organic matter indicating less effective carbonization compared to other feedstocks (Jamiu *et al.*, 2017; Hassan *et al.*, 2021).

Ash Content which representing inorganic residue, was lowest in MHAC ZnCl₂ (7.14%) and highest in RSAC H₂SO₄ (13.14%). ZnCl₂ minimized ash formation across all biomass types, supporting its value in producing pure carbon (Ioannidou & Zabaniotou, 2007; Rahman *et al.*, 2023). High ash in RSAC and MHAC treated with H₂SO₄ reduces adsorption potential.

Sample	Surface Area (m²/g)	Pore Volume (CM³/g)	Pore-siz (CM ³ /g		tribution	Langmuir Surface Area (m²/g)	Iodine Number (mg/g)
	S _{BET}		V Micro	V Meso	V Macro		
CCAC H ₂ SO ₄	351.763	0.310	0.124	0.176	0.089	4,026.220	1,223.5
CCAC HNO ₃	556.473	0.476	0.175	0.266	0.128	4,026.220	932.428
CCAC ZnCl ₂	304.460	0.269	0.147	0.151	0.076	1,749.310	956.62
MHAC H ₂ SO ₄	318.265	0.281	0.112	0.162	0.028	5,227.260	1,154.84
MHAC HNO ₃	387.048	0.353	0.153	0.214	0.114	2,095,585	913
MHAC ZnCl ₂	270.014	0.241	0.98	0.141	0.072	270.014	852.46
RSAC H ₂ SO ₄	329.838	0.149	0.073	0.097	0.046	329.838	813.28
RSAC HNO ₃	434.702	0.388	0.0155	0.224	0.115	432.702	834.62
RSAC ZnCl ₂	281.104	0.253	0.105	0.151	0.077	208.944	804.86

Table 5. Porosity of Activated Carbon

Fixed Carbon which isa key indicator of carbonization efficiency was highest in CCAC H₂SO₄ (82.4%) and MHAC ZnCl₂ (81.12%), while RSAC showed the lowest (68.71-72.41%). This confirms

CC superior carbon retention and suitability for adsorption applications, especially under H₂SO₄ activation (Sulaiman *et al.*, 2022; Ambursa *et al.*, 2023).

The porosity characteristics of activated carbons synthesized from CCAC, MHAC and RSAC using H₂SO₄, HNO₃, and ZnCl₂ activators reveal significant variations in BET surface area, pore volume, pore size distribution, Langmuir surface area, and iodine number highlighting the influence of both precursor and chemical activator on pore architecture are indicated in table 5. From the result, HNO₃ activated samples consistently yielded the highest BET surface areas for CCAC (556.47 m²/g), MHAC (387.05 m²/g), and RSAC (434.70 m²/g) hence, attributed to its strong oxidative action that promotes pore opening through surface functionalization and volatile removal (Gonzalez 2018). Conversely, ZnCl₂ activated samples exhibited the lowest BET surface areas, aligning with its catalytic tendency to form wider but fewer pores, limiting total surface area (Shaikh *et al.*, 2018; Nyamful *et al.*, 2021).

In terms of total pore volume, HNO₃ activation again proved most effective, achieving 0.476 cm³/g in CCAC, 0.353 cm³/g in MHAC, and 0.388 cm³/g in RSAC, with mesopores generally dominant. This indicates its advantage for adsorbing a wide range of molecular sizes. ZnCl₂ showed more mesoporosity but with lower micropore volume, which may hinder adsorption of smaller molecules (Saka, 2012). Pore size distribution analysis revealed that HNO₃ and H₂SO₄ activation tend to favor mesopore and micropore development, respectively, whereas ZnCl₂ activation yields more mesoporous materials, with moderate adsorption capacity (Du *et al.*, 2021). The feedstock's intrinsic properties such as lignin content in corn cob and silica in rice straw also played a role in determining the final porosity (Ioannidou & Zabaniotou, 2007; Ahmad *et al.*, 2015).

Langmuir surface area, indicative of monolayer adsorption capacity, peaked in MHAC H₂SO₄ (5,227.26 m²/g) and CCAC H₂SO₄/HNO₃ (4,026.22 m²/g). These results suggest that H₂SO₄ enables extensive micropore development through dehydration and sulfonation (Feng *et al.*, 2020). In contrast, ZnCl₂ showed markedly lower Langmuir areas, consistent with its reduced microporosity (Song *et al.*, 2013).

Iodine number, a proxy for micropore content and small molecule adsorption, followed similar trends. The highest values were observed for CCAC H₂SO₄ (1,223.5 mg/g) and MHAC H₂SO₄ (1,154.84 mg/g), confirming the effectiveness of sulfuric acid in producing microporous structures (Tubino & Aricetti 2013). In RSAC, HNO₃ activation showed the highest iodine value (834.62 mg/g), although overall values were lower due to silica interference in rice straw (Demiral & Gungor, 2016). The SEM images of the activated carbon synthesized from all the samples presented in figure 2, show a highly porous and irregular surface morphology characterized by the presence of deep crevices and interconnected pores.

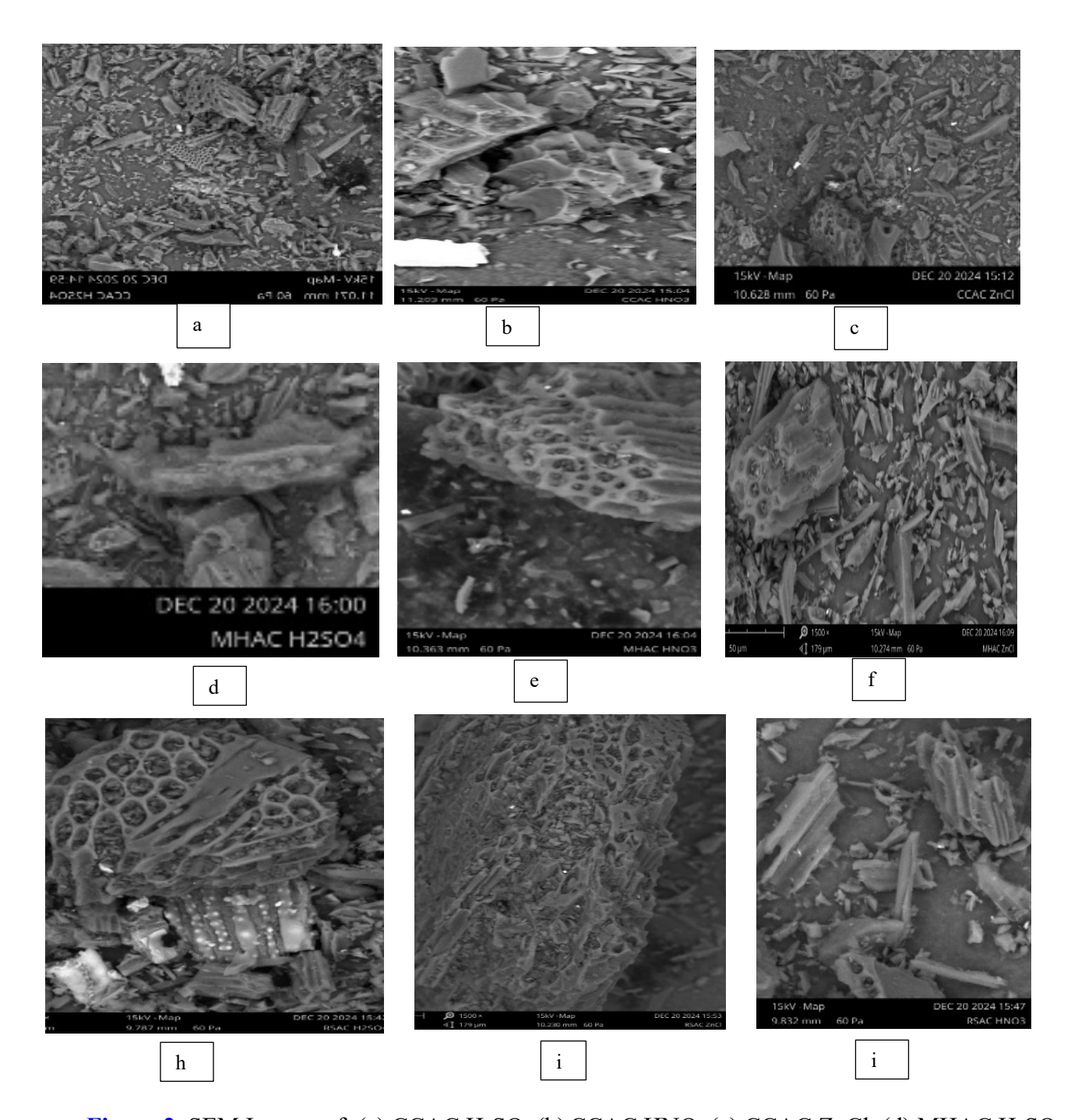


Figure 2. SEM Images of: (a) CCAC H₂SO₄ (b) CCAC HNO₃ (c) CCAC ZnCl₂ (d) MHAC H₂SO₄ (e) MHAC HNO₃ (f) MHAC ZnCl₂ (g) RSAC H₂SO₄ (h) RSAC HNO₃ (i) RSAC ZnCl₂

However, with exception CCAC HNO₃ and RSAC H₂SO₄, all samples appear to have fibrous-like structure with long ridges. For the case of CCAC HNO₃ and RSAC H₂SO₄, a cross-interconnected spongy-like pore was observed. Some studies describe how presence of rough and micro-pores offers more adsorption sites for activated carbon adsorbents (Saka 2012). The difference in pore size and shapes observed from the samples could be as a result of depolymerization and release of volatile substances from the samples during carbonization process thus leading to enhanced porosity (Ali *et al.*, 2020).

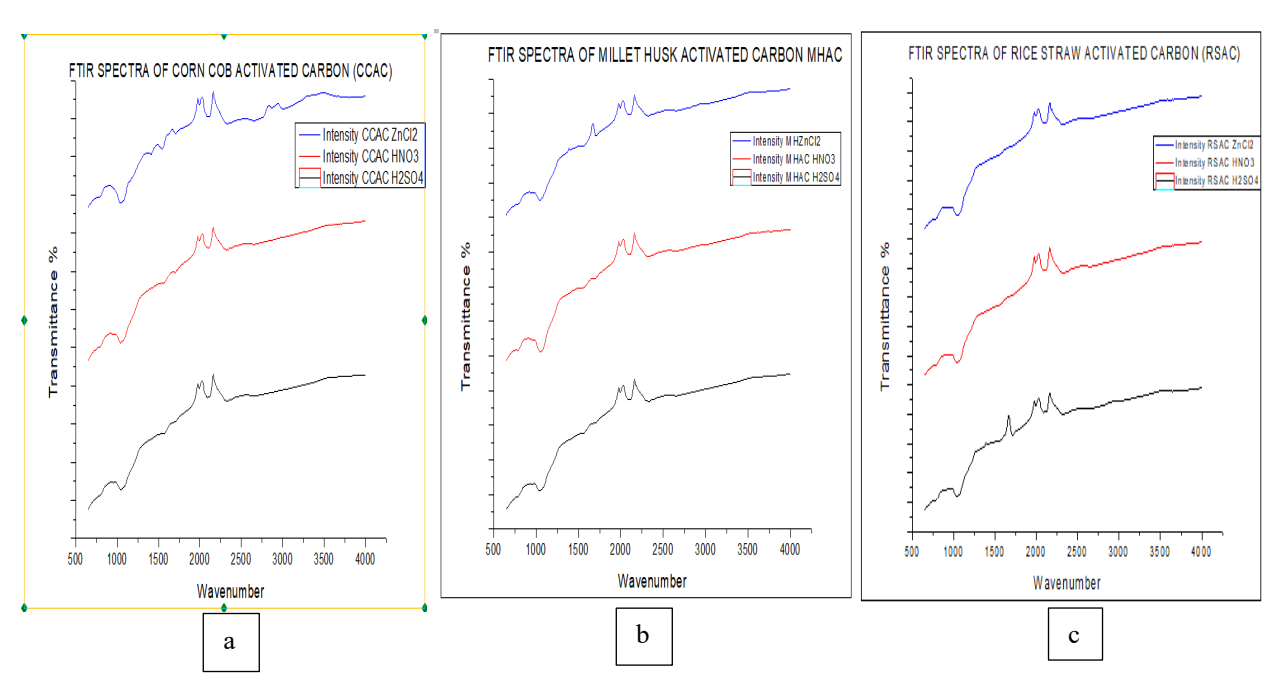


Figure 3. FTIR Spectrum (a) CCAC (b) MHAC (c) RSAC

FTIR analysis presented in **Figure 3** confirmed the presence of diverse functional groups on the surfaces of activated carbons derived from CCAC, MHAC and RSAC reflecting the influence of chemical activating agents H₂SO₄, HNO₃ and ZnCl₂ on surface chemistry and adsorption potential. Across all samples, strong C-O stretching vibrations were observed, indicating the presence of alcohols, ethers, or phenols, which enhance hydrophilicity and favor adsorption of polar species such as dyes and heavy metals (Danish & Ahmad, 2018; Ojedokun & Bello, 2019). Peaks associated with C≡C or C≡N stretching (alkynes or nitriles) were also present, particularly in HNO₃ and ZnCl₂ activated samples, suggesting incorporation of nitrogen functionalities and increased unsaturation, which improve reactivity and adsorption of organic and acidic pollutants (Gao *et al.*, 2013). Moreso, C=O stretching vibrations, representative of carbonyl, carboxyl, or ester groups, were common in all acid-activated samples. These groups provide acidic adsorption sites and contribute to interactions with inorganic contaminants (El-Hendawy, 2009). Peaks associated with O=C=O vibrations were attributed to adsorbed CO₂ or carbonate species, indicating partial oxidation of the carbon surface, beneficial for acidic gas capture (Jiang *et al.*, 2013).

Additionally, several samples exhibited C-H stretching bands related to aliphatic and aromatic hydrocarbons, which suggest retained organic frameworks and contribute to the adsorption of non-polar pollutants (Saucier *et al.*, 2015). Notably, ZnCl₂ activated samples showed multiple bands reflecting aromaticity, conjugation, and residual nitrogen groups, contributing to structural stability and enhanced performance in adsorbing a wide range of contaminants (Ali *et al.*, 2020). Similarly, the presence of O-H stretching bands in certain samples confirmed the existence of hydroxyl groups, known to increase

surface polarity and water affinity, further supporting the carbons' utility in aqueous phase adsorption applications (Guo & Rockstraw, 2007).

Table 6. pH of the Activated Carbon

Activated Carbon	pН
CCAC H ₂ SO ₄	4.8
CCAC HNO ₃	5.3
CCAC ZnCl ₂	6.8
MHAC H ₂ SO ₄	4.4
MHAC HNO ₃	4.9
MHAC ZnCl ₂	7.2
RSAC H ₂ SO ₄	5.5
RSAC HNO ₃	5.8
RSAC ZnCl ₂	7.5

The pH of activated carbon presented in table 6 reflects its surface acidity, which is influenced by both the activating agent and the biomass precursor. In this study, H₂SO₄ treated samples showed the lowest pH values (4.4 -5.5) due to the incorporation of strong acidic groups like sulfonic and carboxylic functionalities (Thommes *et al.*, 2015). HNO₃ activation yielded moderate pH values (4.9 -5.8), attributed to nitro and carboxylic groups that impart milder acidity (Yahya *et al.*, 2015). In contrast, ZnCl₂ activated samples exhibited the highest pH (6.8 -7.5), indicating a more neutral surface, as ZnCl₂ enhances porosity without introducing significant acidity (Kumar *et al.*, 2011; Jami'u *et al.*, 2017).

Conclusion

This study successfully synthesized AC from CC, MH and RS through hydrothermal pretreatment followed by chemical activation using H₂SO₄, HNO₃, and ZnCl₂. The results demonstrate that precursor type and activating agent significantly influence the physicochemical and surface properties of the resulting carbons. CC consistently produced superior yields and higher fixed carbon content compared to MH and RS, indicating its greater suitability as a precursor. Among the activating agents, H₂SO₄ and HNO₃ promoted enhanced porosity and surface functionality, with CCAC H₂SO₄ achieving the highest iodine number (1,223.5 mg/g) and CCAC HNO₃ showing the largest BET surface area (556.5 m²/g). FTIR and SEM analyses confirmed the presence of oxygenated functional groups and well-developed pore structures, both of which are essential for adsorption applications. Overall, CC derived activated

carbons, particularly those activated with H₂SO₄ and HNO₃, demonstrated the best combination of yield, porosity, and functional groups, underscoring their potential as low-cost, sustainable adsorbents for wastewater treatment and environmental remediation. Future studies should extend this work to adsorption performance testing with specific contaminants, kinetic and isotherm modelling, and regeneration studies to fully establish their practical applicability.

Conflict of Interest

The authors declare that the research was conducted in the absence of any commercial or financial relationships that could be construed as a potential conflict of interest.

References

- Abdel-Rahman, G. (2022). Heavy metals, definition, sources of food contamination, incidence, impacts and remediation: A literature review with recent updates, *Egyptian Journal of Chemistry*, 65(1), 419-437. doi: 10.21608/ejchem.2021.80825.4004
- Ahmed, M. J., & Theydan, S. K. (2012). Physical and chemical characteristics of activated carbon prepared by pyrolysis of chemically treated corn cob. *Journal of Analytical and Applied Pyrolysis*, 97, 116–122. https://doi.org/10.1016/j.jaap.2012.06.011
- Ahmed, M. J., & Theydan, S. K. (2012). Physical and chemical characteristics of activated carbon prepared by pyrolysis of chemically treated corn cob. *Journal of Analytical and Applied Pyrolysis*, 97, 116–122. https://doi.org/10.1016/j.jaap.2012.06.011
- Akartasse N., Azzaoui K., Mejdoubi E., Hammouti B., Elansari L.L., Abou-salama M., Aaddouz M., Sabbahi R., Rhazi L. and Siaj M. (2022), Environmental-Friendly Adsorbent Composite Based on Hydroxyapatite/Hydroxypropyl Methyl-Cellulose for Removal of Cationic Dyes from an Aqueous Solution, *Polymers*, 14(11), 2147; https://doi.org/10.3390/polym14112147
- Akinyemi, O., Okon, S. A. (2021). Sustainable synthesis of activated carbon from agro-waste biomass: A review. *Environmental Challenges*, 4, 100129. https://doi.org/10.1016/j.envc.2021.100129
- Ali, R., Aslam, Z., & Shawabkeh, R. A. (2020). BET, FTIR, and RAMAN characterizations of activated carbon from waste oil fly ash. *Turkish Journal of Chemistry*, 44(1), 1–15. https://doi.org/10.3906/kim-1909-8
- Altenor, A. B. (2009). Production of Activated Carbon from Agricultural Residues: A Review. Renewable and Sustainable Energy Reviews, 2009, 13(9), 2452-2465.
- Angon P.B., Islam Md.S., Shreejana K.C., Das A., Anjum N., Poudel A., Suchi S.A. (2024). Sources, effects and present perspectives of heavy metals contamination: Soil, plants and human food chain, *Heliyon*, 10, Issue 7, e28357, https://doi.org/10.1016/j.heliyon.2024.e28357

- Baker R.T. k (2018). Activated Carbon: Manufacture, Properties, and Application by in CRK Press, 2018
- Chen, Y., Xing, L., & Han, L. (2017). Renewable biomass-derived biochars for catalytic applications: A review. *Applied Energy*, 206, 1228–1241. https://doi.org/10.1016/j.apenergy.2017.09.091
- Cheng, W., Yang, D., & Liu, N. (2017). Preparation and characterization of activated carbon from rice straw for heavy metal adsorption. *Journal of Environmental Sciences*, *55*, 220–227. https://doi.org/10.1016/j.jes.2016.08.005
- Danish, M., & Ahmad, T. (2018). A review on utilization of wood biomass as a sustainable precursor for activated carbon production and application. *Renewable and Sustainable Energy Reviews*, 87, 1–21. https://doi.org/10.1016/j.rser.2018.02.003
- Demiral, H., & Gungor, C. (2016). Production of activated carbon from hazelnut shells and its application in wastewater treatment. BioResources, 11(4), 9407–9419.
- Du C, Liu B, Hu J, Li H (2021) Determination of iodine number of activated carbon by the method of ultraviolet–visible spectroscopy. *Mater Lett.*, 285, 129137. doi: j.matlet.2020.129137
- El-Hendawy, A.-N. A. (2009). An insight into the KOH activation mechanism through the production of microporous activated carbon for the removal of Pb²⁺ cations. *Applied Surface Science*, 255(6), 3723–3730. https://doi.org/10.1016/j.apsusc.2008.10.034
- El-Sayed, S. A., & Bandosz, T. J. (2015). Rice husk-derived activated carbon modified with HNO₃ for enhanced adsorption of heavy metals. *Journal of Hazardous Materials*, 286, 456–465.
- Feng P, Li J, Wang H, Xu Z (2020) Biomass-based activated carbon and activators: preparation of activated carbon from corncob by chemical activation with biomass pyrolysis liquids. *ACS Omega* 5(37), 24064–24072. https://doi.org/10.1021/acsomega.0c03494
- González, J. F., Román, S., Encinar, J. M., & Martínez, G. (2009). Pyrolysis of various biomass residues and char characterization. *Fuel Processing Technology*, 89(9), 917–924. https://doi.org/10.1016/j.fuproc.2008.10.002
- González-García P. (2018) Activated carbon from lignocellulosics precursors: a review of the synthesis methods, characterization techniques and applications. In *Renew Sustain Energy Rev* 82, 1393–1414. https://doi.org/10.1016/j.rser.2017.04.117
- Guo, Y., & Rockstraw, D. A. (2007). Physicochemical properties of carbons prepared from pecan shell by phosphoric acid activation. *Bioresource Technology*, 98(8), 1513–1521.
- Gupta, V. K., Carrott, P. J. M., Ribeiro Carrott, M. M. L., & Suhas. (2015). Low-cost adsorbents: Growing approach to wastewater treatment—a review. *Critical Reviews in Environmental Science and Technology*, 39(10), 783–842. https://doi.org/10.1080/10643380801977610

- Hassan, H., Lim, J. K., & Pang, Y. L. (2021). A review on the characterization and applications of activated carbon synthesized from biomass waste via chemical activation processes. *Journal of Cleaner Production*, 289, 125677. https://doi.org/10.1016/j.jclepro.2020.125677
- Ioannidou O., Zabaniotou A. (2007). Agricultural residues as precursors for activated carbon production—A review. *Renewable and Sustainable Energy Reviews*, 11(9), 1966-2005. https://doi.org/10.1016/j.rser.2006.03.013
- Jamiu W, Adebayo G.B, Amigun A.T, Jimoh A.A, Musa R.T, and Garuba B. (2017) Effectiveness of activated carbon from low-cost agricultural wastes: physico-chemical and spectroscopic characterization *International Research Journal of Agricultural Science and Technology*, 1(2), 15-21, http://www.ediblejournals.org/IRJAST
- Karim S., Aouniti A., M. Taleb, F. El Hajjaji, C. Belbachir, I. Rahhou, Achmit M., Hammouti B. (2019), Evaluation of heavy metal concentrations in seven Commercial marine Fishes caught in the Mediterranean coast of Morocco and their associated health risks to consumers, *Journal of Environment and Biotechnology Research*, 8 (1), 1-13, DOI: 10.5281/zenodo.2529361
- Konan A. T. S., Richard R., Andriantsiferana C., Yao K. B., Manero M.-H. (2020). Recovery of borassus palm tree and bamboo waste into activated carbon: application to the phenolic compound removal, *J. Mater. Environ. Sci.*, 11(10), 1584-1598
- Li, W., Zhang, L., Peng, J., Li, N., Zhu, X., & Guo, S. (2016). Effects of carbonization temperatures on characteristics of porosity in biomass-based activated carbon. *Biomass and Bioenergy*, 49, 1-7. https://doi.org/10.1016/j.biombioe.2016.03.012
- Lua, A. C., & Yang, T. (2014). Effects of activating agent and activation temperature on the properties of activated carbon prepared from pistachio-nut shells. *Journal of Colloid and Interface Science*, 274(2), 594–601. https://doi.org/10.1016/j.jcis.2004.02.053
- Mahmoud, A. A., Ahmed, E. A., & Wahba, A. M. (2018). Corn cob-based activated carbon prepared by chemical activation for the removal of heavy metals from wastewater. *Environmental Nanotechnology, Monitoring & Management, 10*, 360–365.
- Murtala M. Ambursa, S. Y. Haruna, Yakubu Yahaya, A. Muhammad, A. B. Muhammad (2023) Synthesis and Characterization of Activated Carbon Derived from *Pennisetum glaucum* Millet Waste for Adsorption Properties. *International Journal of Modern Chemistry*, 15(1), 42-50
- Nguyen T.A.H., Ngo H.H., Guo W.S. (2013). Applicability of Agricultural Waste and by Products for Adsorptive Removal of Heavy Metals from Waste Water (Review). *Bioresour Technol*. 148, 574-585
- Nisar, J., Memon, S., Jatoi W. (2020). Activated carbon from agricultural by-products: Preparation and

- applications. Bioresource Technology Reports, 11, 100489. Doi: j.biteb.2020.100489
- Nyamful A., Nyogbe E.K., Mohammed L., Zainudeen M.N., Darkwa S.A., Phiri I., Mohammed M., Ko J.M. (2021). Processing and characterization of activated carbon from coconut shell and palm kernel shell waste by H₃PO₄ activation. *Ghana J. Sci.* 61(2), 91–104. https://doi.org/10.4314/gjs.v61i2.9
- Ojedokun, A. T., & Bello, O. S. (2019). Corn cob and its derivatives as promising adsorbents for the removal of pollutants from wastewater: A critical review. *Renewable and Sustainable Energy Reviews*, 89, 223–247. https://doi.org/10.1016/j.rser.2018.03.015
- Opia, A.C.; Hamid, M.K.B.A.; Syahrullail, S.; Rahim, A.B.A.; Johnson, C.A.N. (2021) Biomass as a potential source of sustainable fuel, chemical and tribological materials Overview. *Mater. Today Proc.* 39, Part 2, 922-928, https://doi.org/10.1016/j.matpr.2020.04.045.
- Rahman, M. A., Islam, M. A., & Khandaker, S. (2023). Comparative analysis of chemical activators on the pore structure and adsorption efficiency of biomass-derived activated carbon. *Materials Today: Proceedings*, 74, 2434–2442. https://doi.org/10.1016/j.matpr.2022.08.074
- Sabbahi R., Azzaoui K., Hammouti B., Saoiabi S. (2022), A global Perspective of Entomopathogens as Microbial Biocontrol Agents of Insect Pests, *Journal of Agriculture and Food Research*, 10, 100376. https://doi.org/10.1016/j.jafr.2022.100376
- Saheed, I., Adekola, F., & Olatunji, G. (2017). Sorption Study of Methylene Blue on Activated Carbon Prepared from *Jatropha curcas* and *Terminalia catappa* Seed Coats. *Journal of the Turkish Chemical Society, Section A: Chemistry*, 4(1), 375–394.
- Saka C. (2012) BET, TG-DTG, FT-IR, SEM, iodine number analysis and preparation of activated carbon from acorn shell by chemical activation with ZnCl₂. *J Anal Appl Pyrol* 95, 21–24. https://doi.org/10.1016/j.jaap.2011.12.020
- Salahat A., Hamed O., Deghles A., Azzaoui K., Qrareya H., Assali M., Mansour W., Jodeh S., Haciosmanoğlu G.G., Can, Z.S., Hammouti B., Nandiyanto A.B.D., Ayerdi-Gotor A., Rhazi L. (2023). Olive Industry Solid Waste-Based Biosorbent: Synthesis and Application in Wastewater Purification. *Polymers*, 15, 797. https://doi.org/10.3390/polym15040797
- Saucier, C., Adebayo, M. A., Lima, E. C., *et al.* (2015). Microwave-assisted activated carbon from cocoa shell as adsorbent for removal of sodium diclofenac and nimesulide from aqueous effluents. *Journal of Hazardous Materials*, 289, 18–27. doi: 10.1016/j.jhazmat.2015.02.059
- Shah A.M., Zhang H., Shahid M., Ghazal H., *et al.* (2025). The Vital Roles of Agricultural Crop Residues and Agro-Industrial By-Products to Support Sustainable Livestock Productivity in Subtropical Regions. *Animals*. 15(8), 1184. https://doi.org/10.3390/ani15081184

- Shaikh R.B., Saifullah B., urRehman F., Shaikh R.I. (2018). Greener method for the removal of toxic metal ions from the wastewater by application of agricultural waste as an adsorbent. *Water* (Switzerland) 10, 10. https://doi.org/10.3390/w10101316
- Song X., Zhang Y., Yan C., Jiang W., Chang C. (2013). The Langmuir monolayer adsorption model of organic matter into effective pores in activated carbon. *J Colloid Interface Sci* 389(1), 213–219. https://doi.org/10.1016/j.jcis.2012.08.060
- Sulaiman, F. R., Rashid, S. A. (2020). Agricultural waste materials as potential sources for activated carbon production: A review. *Materials Today: Proceedings*, 31, 730–736. https://doi.org/10.1016/j.matpr.2020.02.469
- Sulaiman, S. K., Umar, H., Yusuf A.A. (2022). Synthesis and characterization of activated carbon from agricultural residues for wastewater treatment applications. *Environmental Nanotechnology, Monitoring & Management, 18,* 100687. https://doi.org/10.1016/j.enmm.2022.100687
- Sun, J., Xiao, C., Wang, D., Wang, Y., & Li, W. (2018). Effect of chemical activation agents on the pore structure and adsorption performance of rice straw-based activated carbon. *Environmental Technology*, 39(6), 797–806. https://doi.org/10.1080/09593330.2017.1317365
- Thommes, M., Kaneko, K., Neimark, A. V., Olivier, J. P., Rodriguez-Reinoso, F., Rouquerol, J., & Sing, K. S. W. (2015). Physisorption of gases, with special reference to the evaluation of surface area and pore size distribution (IUPAC Technical Report). *Pure and Applied Chemistry*, 87(9-10), 1051-106
- Tsade H., Ananda Murthy H. C. and Muniswamy D. (2020). Bio-sorbents from Agricultural Wastes for Eradication of Heavy Metals: A Review, *J. Mater. Environ. Sci.*, 11(10), 1719-1735
- Tubino M., Aricetti J.A. (2013). A green potentiometric method for the determination of the iodine number of biodiesel. *Fuel* 103, 1158–1163. https://doi.org/10.1016/j.fuel.2012.10.011
- Vassilev, S. V., Vassileva, C. G., & Vassilev, V. S. (2010). An overview of the chemical composition of biomass. *Fuel*, 89(5), 913–933. https://doi.org/10.1016/j.fuel.2009.10.022
- Zhang H., Wang X., Jiang D. (2023). Advanced applications of rice straw-derived activated carbon: A comprehensive review. *Renewable Energy*, 200, 658–671. doi: 10.1016/j.renene.2022.10.048

(2026); www.mocedes.org/ajcer